

Experimental and theoretical lifetimes and transition probabilities for spectral lines in Nb II

H. Nilsson¹, L. Engström², H. Lundberg², H. Hartman^{1,3}, P. Palmeri⁴, and P. Quinet^{4,5}

¹ Lund Observatory, Lund University, Box 43, 22100 Lund, Sweden
e-mail: hampus.nilsson@astro.lu.se

² Department of Physics, Lund University, Box 118, 22100 Lund, Sweden

³ Materials Science and Applied Mathematics, Malmö University, 20506 Malmö, Sweden

⁴ Physique Atomique et Astrophysique, Université de Mons, 7000 Mons, Belgium

⁵ IPNAS, Université de Liège, 4000 Liège, Belgium

Received 4 April 2019 / Accepted 30 May 2019

ABSTRACT

Aims. We have measured and calculated lifetimes of high lying levels in Nb II, and derived absolute transition probabilities by combining the lifetimes with experimental branching fractions.

Methods. The lifetimes were measured using time-resolved laser-induced fluorescence in a two-photon and two-step excitation scheme. The branching fractions were measured in intensity calibrated spectra from a hollow cathode discharge, recorded with a Fourier transform spectrometer. The calculations were performed with the relativistic Hartree–Fock method including core polarization.

Results. We report experimental lifetimes of 13 levels in the $4d^3(^4F)5d$ and $4d^3(^4F)6s$ subconfigurations, at an energy around $70\,000\text{ cm}^{-1}$. By combining the lifetimes with experimental branching fractions absolute transition probabilities of 59 lines are derived. The experimental results are compared with calculated values.

Key words. atomic data – methods: laboratory: atomic – techniques: spectroscopic

1. Introduction

Niobium was discovered in 1801 by the British chemist Charles Hatchett. The element was discovered in the mineral columbite, and Hatchett gave the element the name columbium (Cb). In 1844 Heinrich Rose reported two new elements, niobium, and penopium. However, Jean-Charles de Marignac showed that the elements columbium, niobium and penopium were in fact all the same. The name columbium was in use until 1949 when niobium was adopted as the official name of element number 41. The Swedish chemist Christian Blomstrand is believed to be the first one to isolate niobium. The fascinating history of niobium, columbium, pelopium, and tantalum and Charles Hatchett can be found in Griffith & Morris (2003).

Niobium is a key element to understand and probe the slow-neutron-capture process (the s-process). Niobium is monoisotopic (^{93}Nb) and believed to be mainly produced by β decay of ^{93}Zr , with a half-life of $\tau_{1/2} = 1.53 \times 10^6$ yr. The probability of ^{93}Zr capturing a neutron and producing ^{94}Zr is larger than that of ^{93}Zr decaying to ^{93}Nb as long as the s-process is ongoing. Hence the niobium abundance can give the time since the s-process ended (Smith & Lambert 1984). Furthermore, by comparing the ratios $^{93}\text{Zr}/^{93}\text{Nb}$ and $^{99}\text{Tc}/^{99}\text{Ru}$ it is possible to determine the s-process temperature and the time since the s-process started (Neyskens et al. 2015).

In 1935 Meggers & Schribner (1935) published a paper reporting the term analysis of the first two spectra, Cb I and Cb II (arc and spark) of columbium, including 2000 lines combining 60 levels in Cb II. The analysis was extended by Humphreys & Meggers (1945) who reported 183 levels in Cb II. In Iglesias (1954) a study of the vacuum ultraviolet spectrum was

reported, identifying 20 new energy levels and 330 spectral lines as belonging to Nb II (this is the first term analysis paper using the name niobium instead of columbium). The most recent term analysis of Nb II is reported by Ryabtsev et al. (2000), based on spectra recorded with Fourier transform spectroscopy. A total of 353 energy levels in Nb II are presently known from the work reported in these papers.

Experimental transition probabilities in Nb II have been reported by Hannaford et al. (1985), by combining radiative lifetimes of 27 levels with branching fractions (BFs) derived from the work of Corliss & Bozman (1962). Nilsson & Ivarsson (2008) reported transition probabilities for 145 lines combining BFs measured in Fourier transform spectra with the lifetimes reported by Hannaford et al. (1985). In Nilsson et al. (2010) additional transition probabilities were reported for lines from the $4d^3\ 5p$ configuration derived from lifetimes combined with BFs, along with new theoretical calculations.

Niobium has one stable isotope, ^{93}Nb , which has an odd number of nucleons. Due to the nuclear spin $I = 9/2$ and a large magnetic moment, $\mu = 6.1705\ \mu_N$ (Mills et al. 1988), many of the spectral lines show large hyperfine structure (hfs). Experimental measurements of hfs has been reported by Young et al. (1995) and Nilsson & Ivarsson (2008). However, none of the lines reported in the present work are noticeably affected by hfs.

In this work we report experimental transition probabilities for 59 lines originating from 13 levels in the $4d^3(^4F)5d$ and $4d^3(^4F)6s$ subconfigurations, derived by combining branching fractions and radiative lifetimes. These new data are compared with semi-empirical calculations performed using a relativistic Hartree–Fock model including core-polarization effects.

2. Laboratory measurements

2.1. Lifetimes

The spectrum and term system of Nb II have been thoroughly investigated by Ryabtsev et al. (2000). This work was essential not only to find the investigated levels but also to check for possible blending, as discussed below. The ground term in Nb II is the even $4d^4\ ^5D$, with levels between 0 and 1200 cm^{-1} , and the second lowest even term is $4d^3(^4F)5s\ ^5F$ between 2300 and 4150 cm^{-1} . To reach the investigated high lying even $5d$ and $6s$ levels, between $68\,000$ and $73\,200\text{ cm}^{-1}$, we employed either two-photon excitations using a single laser or a two-step procedure where the first laser excited intermediate odd levels in the $4d^3(^4F)5p\ ^5G$ term from which the second laser reached the $5d$ and $6s$ levels. Figure 1 illustrates the levels and wavelengths involved, and Table 1 gives the detailed excitation scheme for each level.

The experimental setup for two-photon and two-step measurements at the high-power laser facility at the University of Lund is described in detail in Engström et al. (2014) and Lundberg et al. (2016) and only the most important details will be given here. The setup includes three Nd:YAG lasers operating at 10 Hz. The frequency-doubled output of one of them (Continuum Surelite) is focused on a rotating niobium target in a vacuum chamber with a pressure of about 10^{-4} mbar to produce the niobium ions through laser ablation. Interactions with the electrons in the created plasma also excite the even $4d^4$ and $4d^35s$ configurations, which contain the starting levels in our experiments.

For the two-step measurements, the second Nd:YAG (Continuum NY-82) laser pumps a dye laser (Continuum Nd-60) which, after frequency-doubling, produces a 10 ns long pulse for the first excitation to the odd $4d^3(^4F)5p\ ^5G$ levels. A similar laser combination is used for the second step, but here the output of the Nd:YAG laser is temporally compressed using Brillouin scattering in water before pumping the dye laser. The frequency-doubled light from the dye laser is then passed through a tube with hydrogen gas where a Stokes shift of 4153 cm^{-1} could be added. The final length, full width at half maximum (FWHM), of the second step pulse was about 1 ns.

Both laser pulses intersected the niobium plasma from the same direction at right angles to the ablation laser a few millimeter above the niobium target. The timing between the two excitations is very important and adjusted so that the second step laser coincided in time with the maximum fluorescence from the intermediate level. Because of the difference in pulse length between the two lasers this ensures that the intermediate level population is constant during the second excitation. For the two-photon measurements only the short pulses from the second laser were used.

The fluorescence from the excited levels was observed with a small f/8 monochromator, with its $120\ \mu\text{m}$ wide entrance slit parallel to the excitation lasers, in a direction perpendicular to all three laser beams. The observed line width (FWHM) was 0.5 nm in the second spectral order. The time varying signal was registered with a microchannel-plate photomultiplier (Hamamatsu R3809U) with a rise time of 0.15 ns, and digitized by a Tektronix DPO 7254 oscilloscope in time intervals of 50 ps. A second channel on the oscilloscope sampled simultaneously the temporal shape of the short-pulsed (1 ns) laser obtained from a fast photodiode. Each decay curve and pulse shape was averaged over 1000 laser shots. Between 10 and 20 decay curves were recorded for each level. The lifetimes were determined by fitting a single exponential decay, convoluted by the measured shape of the second step laser, and a constant background using the

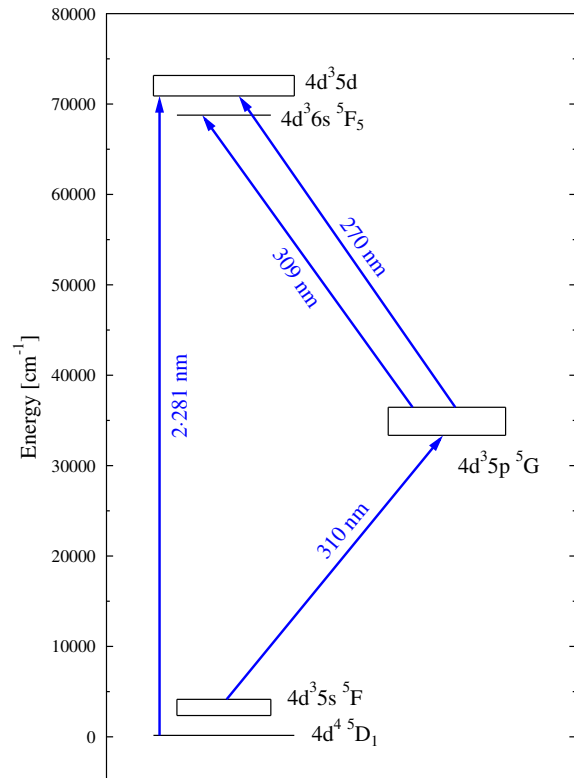


Fig. 1. Schematic term system for Nb II showing the investigated levels and the typical wavelengths used for the two-photon and two-step excitations.

software DECFIT (Palmeri et al. 2008). In the two-photon case, the square of the measured excitation pulse was used.

In the two-step measurements some corrections of the recorded decay curves were necessary before the fitting procedure. In the case of $5d\ ^5H_{6,7}$ the only sufficiently intense decay channels were the same as those used for the second step excitation. This resulted in a contamination of the decay by scattered laser light. However, this effect was taken care of by recording a decay curve for the second laser either at a wavelength slightly off resonance or with the first step laser blocked. This measurement was then subtracted from the observed primary decay before the lifetime extraction. Figure 2 illustrates this problem for $5d\ ^5H_6$, which was the worst case observed. Another problem was encountered in most cases because the very intense and long-lived fluorescence from the intermediate level could produce a small but noticeable contribution in the measured decay channel even at substantial wavelength differences. Similar to the previous example, this could be handled by recording and subtracting the signal from the intermediate level with the second step laser blocked. Finally, for both two-photon and two-step measurements, uncorrectable blending problem may arise from cascades, that is intermediate levels being populated from the level under investigation that in turn decay with wavelengths close to the investigated decay channel. This problem precluded for example the measurement of the $5d\ ^5G_4$ level. To search for such effects, detailed spectroscopic studies, such as the one by Ryabtsev et al. (2000), are essential.

The excitation schemes employed and the final experimental lifetimes are presented in Table 1. The quoted uncertainties are based on the variations between the repeated measurements that include tests to ascertain the absence of systematic effect. Examples of the latter effects are the variations in the lifetimes with

Table 1. Experimental details and the measured and calculated lifetimes of the levels in Nb II.

Level	$E^{(a)}$ [cm ⁻¹]	Intermediate level		Excitation λ_{air} [nm]	$\lambda_{\text{obs}}^{(b)}$ [nm]	Method ^(c)	τ_{exp} [ns]	τ_{theory} [ns]	
		Term	$E^{(a)}$ [cm ⁻¹]					This work	Kurucz ^(d)
6s ⁵ F ₅	68 772.9	5p ⁵ G ₆	36 455.5	309.3	325	2 ω	2.55 ± 0.10	2.54	2.79
5d ⁵ H ₃	70 895.5			282.6	266	2 γ , 2 ω	1.65 ± 0.20	1.72	1.65
5d ⁵ H ₅	71 684.9	5p ⁵ G ₄	34 632.0	269.8	270, 293	2 ω + AS	1.95 ± 0.15	1.82	1.76
5d ⁵ H ₆	72 231.7	5p ⁵ G ₅	35 474.2	272.0	272	2 ω + AS	1.95 ± 0.15 ^e	1.86	1.77
5d ⁵ H ₇	72 861.3	5p ⁵ G ₆	36 455.5	274.6	274	2 ω + AS	1.75 ± 0.10 ^e	1.89	1.77
5d ⁵ G ₅	72 460.7	5p ⁵ G ₅	35 474.2	270.3	286	2 ω + AS	2.1 ± 0.2	2.08	2.02
5d ⁵ G ₆	73 161.1	5p ⁵ G ₆	36 455.5	272.4	285	2 ω + AS	2.1 ± 0.2	2.11	2.05
5d ⁵ P ₁	70 956.0			282.4	299	2 γ , 2 ω	2.10 ± 0.15	2.11	2.11
5d ⁵ P ₃	72 125.2	5p ⁵ G ₄	34 632.0	266.6	295	2 ω + AS	2.00 ± 0.15	2.03	1.98
5d ⁵ F ₁	71 196.1			281.5	275	2 γ , 2 ω	2.20 ± 0.15	1.92	1.94
5d ⁵ F ₃	72 183.1	5p ⁵ G ₄	34 632.0	266.2	280	2 ω + AS	2.00 ± 0.15	1.96	1.98
5d ⁵ F ₄	72 624.9	5p ⁵ G ₅	35 474.2	269.1	285	2 ω + AS	2.00 ± 0.15	1.98	1.95
5d ⁵ F ₅	73 115.4	5p ⁵ G ₆	36 455.5	272.7	285	2 ω + AS	1.95 ± 0.15	2.00	1.96

Notes. ^(a)Ryabtsev et al. (2000). ^(b)All fluorescence measurements were performed in the second spectral order. ^(c)2 ω means the second harmonic of the dye laser, AS means one added Stokes shift (4153 cm⁻¹) and 2 γ means two-photon excitation. ^(d)Semi-empirical superposition-of-configurations calculation by Kurucz (2017). ^(e)Corrected for scattered light from the second step laser.

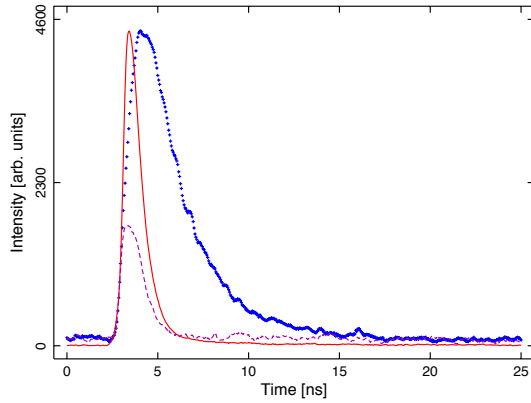


Fig. 2. Measured decay curve for the 4d³5d ⁵H₆ level (+) and the recorded second step laser pulse (–). The dashed curve is a recording of the scattered light from the second step laser at a slightly detuned wavelength. This measurement is then subtracted from the real decay before the lifetime determination. The actual measurement extends to 40 ns.

and without the small correction for the background contribution from the intermediate levels, discussed above, and the search for saturation effects by inserting a varying number of neutral density filters in the second step laser beam. Furthermore, possible flight effects (Sikström et al. 2002) were investigated by varying the delay between the ablation and excitation lasers, which results in ions with different velocities arriving in the interaction zone at a fixed distance from the target.

2.2. Branching fractions and transition probabilities

The branching fraction (BF) of a line is defined as the transition probability of the line divided by the sum of transition probabilities for all lines from the same upper level, that is the inverse of the lifetime (τ). Hence, if one can measure the intensity of all transitions from one upper level, transition probabilities can be derived by combining the BFs with radiative lifetimes according to $BF_{ul} = I_{ul} / \sum_{k=1} I_{uk}$ and $A_{ul} = BF_{ul} / \tau_u$. To convert the transition probabilities to oscillator strengths (f), the following relation can be used: $g_l f_{lu} = (\lambda / 258.27)^2 g_u A_{ul}$, where $g_{l(u)}$ is the statistical weight of the lower (upper) level, with λ in nm and A in (ns)⁻¹.

However, some lines can be too weak to be measured, but the total BF of all missing lines can be estimated from theoretical calculations. This correction is called the residual and is given in Table A.1 for each level.

The niobium spectra were produced in a hollow cathode discharge with a mixture of neon and argon as carrier gas (at a current of 0.6 A and a pressure of 1 Torr), and recorded using the Lund Observatory Chelsea Instruments FT500 UV Fourier transform spectrometer, with a resolution of 0.035 cm⁻¹. Two spectra were used. The first, covering the wavenumber region 20 000–40 000 cm⁻¹ (250–500 nm), was recorded with a Hamamatsu R955 optical photomultiplier tube. The second spectrum (28 000–56 000 cm⁻¹, 180–360 nm) was recorded with a Hamamatsu R166 solar blind photomultiplier tube. The spectra were intensity calibrated using branching ratios in argon (from 20 000 to 35 000 cm⁻¹, 290–500 nm) reported by Whaling et al. (1993), and a deuterium lamp calibrated by Physicalisch-Technische Bundesanstalt, Berlin, Germany (30 000–50 000 cm⁻¹, 200–330 nm). The calibration procedure is further discussed in Sikström et al. (2002).

The uncertainties in the BFs include the uncertainty in the intensity measurements and the uncertainty in the intensity calibration, not only in the line itself, but also in the other lines from the same upper level, as they influence the derived value of the BF. The method to estimate uncertainties is described in detail in Sikström et al. (2002). The derived BFs and log(gf) values are given in Table A.1. The BFs are compared with theoretical values from this work and values from Kurucz (2017). In addition, we present the uncertainties both in the BFs and in the gf -values. The uncertainty in the gf -values includes the uncertainty both in the BF and the lifetime.

In most cases the lines were easy to identify thanks to the thorough analysis by Ryabtsev et al. (2000). However, we found a few lines that were blended or misidentified. The transition 4d³(⁴F)5p ⁵F₃ – 4d³(⁴F)5d ⁵P₃ at 34 748.346 cm⁻¹ (287.7 nm) is blended with a weak hfs pattern, as seen in Fig. 3. The intensity of the line is corrected by measuring the intensity of the adjacent hfs components to estimate the blending contribution. The correction changed the BF of this line from 0.40 to 0.35.

The line at 25 770.230 cm⁻¹ (387.9 nm) is identified by Ryabtsev et al. (2000) as 4d³(²H)5p ³H₄ – 4d³(⁴F)5d ⁵F₅. However, as suggested by Nilsson et al. (2010), this is probably the

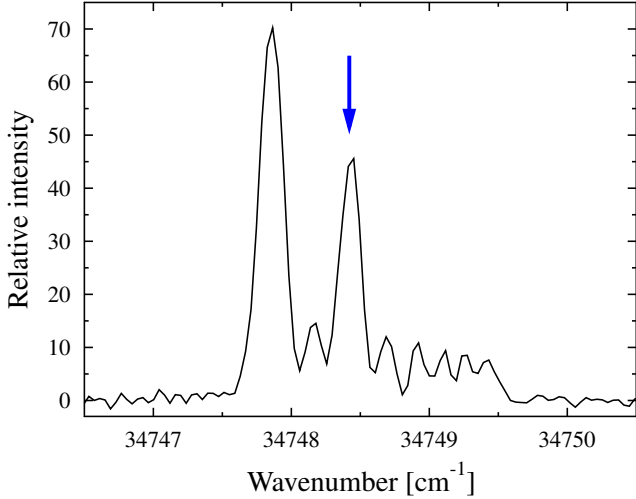


Fig. 3. $4d^3(^4F)5p\ ^5F_3 - 4d^3(^4F)5d\ ^5P_3$ transition, marked with the arrow. The line is blended with the wide hfs pattern of an unidentified line. The blending intensity is estimated with the adjacent hfs components (see text).

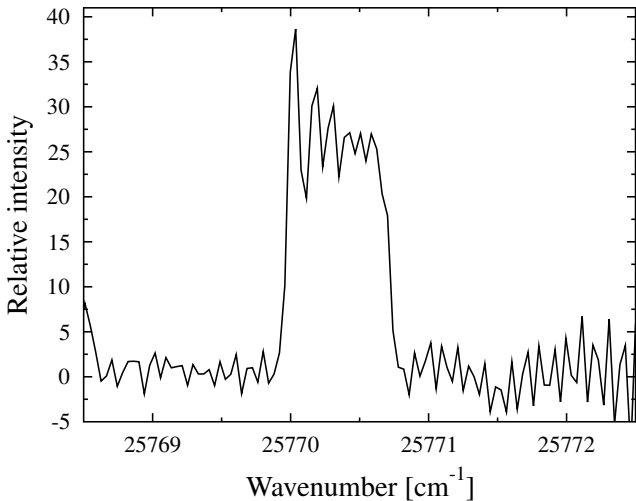


Fig. 4. $4d^4\ a^1G_4 - 4d^3(^4F)5p\ z^3F_4$ transition. The line is wrongly assigned as $4d^3(^2H)5p\ ^3H_4 - 4d^3(^4F)5d\ ^5F_5$ transition by Ryabtsev et al. (2000) (see text).

$4d^4\ a^1G_4 - 4d^3(^4F)5p\ z^3F_4$ transition instead, which has a Ritz wavenumber of $25\ 770.263\ \text{cm}^{-1}$. Furthermore, this identification is strengthened by analysing the hfs pattern (as can be seen in Fig. 4) of the line, which is consistent with the splittings in the two levels, $4d^4\ a^1G_4$ and $4d^3(^4F)5p\ z^3F_4$, reported by Nilsson & Ivarsson (2008).

The line at $32\ 554.352\ \text{cm}^{-1}$ (307.1 nm) is identified by Ryabtsev et al. (2000) as $4d^3(^4F)5p\ ^3F_4 - 4d^3(^4F)5d\ ^5F_5$. However, this coincides with the $4d^4\ a^1G_4 - 4d^3(^2H)5p\ ^3H_4$ transition (with the Ritz wavenumber $32\ 554.359\ \text{cm}^{-1}$) which, according to our calculations, has a transition probability that is orders of magnitude larger. We therefore conclude that the two lines $25\ 770.230\ \text{cm}^{-1}$ and $32\ 554.352\ \text{cm}^{-1}$ are misidentified by Ryabtsev et al. (2000), and we have excluded them in the analysis of the level $4d^3(^4F)5d\ ^5F_5$ at $73\ 115.352\ \text{cm}^{-1}$.

In most cases the residual is small (between 0.4 and 4.1%). However, for the $4d^3(^4F)5d\ ^5P_1$ and $4d^3(^4F)5d\ ^5F_1$ transitions, the residuals are larger 14.4 and 31.3%, respectively). This is

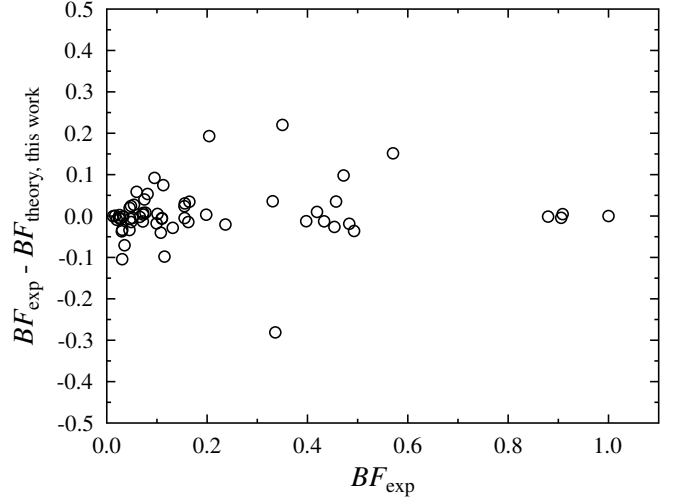


Fig. 5. Comparison between our experimental BFs and theoretical values.

because that the population is proportional to the statistical weight, $g = 2J + 1$, so lines from levels with $J = 1$ have a lower signal to noise ratio, and some of the lines therefore become too weak to be measured. However, the lines that are measured are in good agreement with the theoretical values, if scaled with the residual. The uncertainties for these two levels will perhaps be overestimated as the residual is given an uncertainty of 50%.

For the levels $4d^3(^4F)5d\ ^5P_3$ and $4d^3(^4F)5d\ ^5F_3$, both $J = 3$, a poor agreement between experiment and theory is seen. We find no experimental reason for this, but it can be noted that the two different calculations are not in agreement for these two levels. Because of the poor agreement between experiment and theory we have not included residuals for these levels. This may overestimate the BFs from these levels slightly.

3. Semi-empirical calculations

The experimental radiative parameters measured in the present work are compared with theoretical results obtained using the pseudo-relativistic Hartree–Fock (HFR) method of Cowan (1981) modified to take core-polarization effects (HFR+CPOL) into account, as described for example by Quinet et al. (1999, 2002). The calculations are based on the same physical model as the one assumed to be best (referred to as HFR(B)) in our previous work on Nb II (Nilsson et al. 2010). As a reminder, in this model the intravalence interactions were considered by explicitly including the following multi-configuration expansions: $4d^4 + 4d^35s + 4d^36s + 4d^35d + 4d^25s^2 + 4d^25p^2 + 4d^25s6s + 4d^25s5d + 4d^24f5p + 4d^25p5f + 4d^26s^2 + 4d^25d^2 + 4d^25d6s + 4d^25p6p$ for the even parity, and $4d^35p + 4d^36p + 4d^34f + 4d^35f + 4d^25s5p + 4d^25s6p + 4d^24f5s + 4d^24f5d + 4d^25s5f + 4d^25p6s + 4d^25p5d + 4d^26s6p$ for the odd parity. Using the well-established least-squares approach that minimizes the differences between the calculated and the available experimental energy levels published by Ryabtsev et al. (2000), some radial parameters were optimized according to the methodology described in detail by Nilsson et al. (2010). The core-polarization effects were first estimated using the dipole polarizability corresponding to the ionic Nb IV core given in Fraga et al. (1976), $\alpha_d = 5.80a_0^3$, while the cut-off radius (r_c) was chosen to be the mean value $\langle r \rangle$ of the outermost 4d core orbital, $r_c = 1.85a_0$. Using these two parameters, we found that our calculated lifetimes were systematically

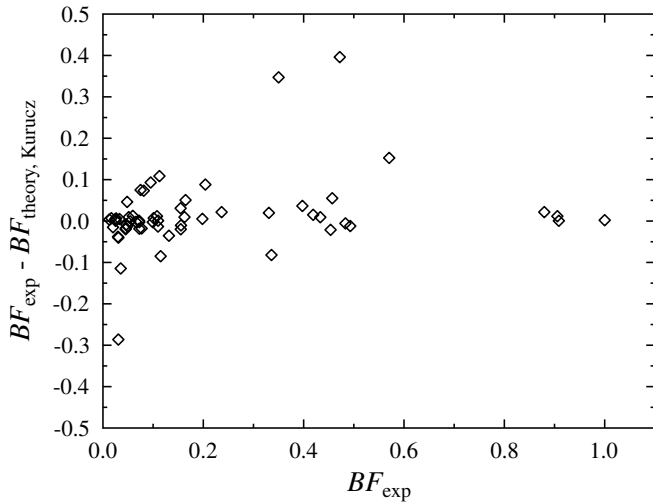


Fig. 6. Comparison between our experimental BFs and theoretical values from Kurucz (2017).

a few percent longer than those measured in the present work for $4d^36s$ and $4d^35d$ levels. Therefore, we adjusted semi-empirically the dipole radial integrals of the $4d^35p - 4d^36s$ and $4d^35p - 4d^35d$ transitions to fit the calculations to the experimental lifetimes. This gave rise to the values $\langle 5p|r|6s \rangle = -2.64$ a.u. and $\langle 5p|r|5d \rangle = -5.74$ a.u., that being respectively 6% and 9% larger than the values obtained using the HFR(B) model considered in our previous paper (Nilsson et al. 2010).

The calculated lifetimes are compared with the experimental measurements in Table 1. We can clearly note that our calculated values fall within the experimental uncertainties, the average ratio $\tau_{\text{Calc}}/\tau_{\text{Exp}}$ being equal to 0.99 ± 0.05 where the uncertainty represents the standard deviation from the mean. This agreement is similar to (but slightly better than) the one obtained when comparing the theoretical data from Kurucz (2017) with the experimental lifetimes ($\tau_{\text{Kurucz}}/\tau_{\text{Exp}} = 0.98 \pm 0.06$). In Table A.1, the BFs calculated in the present work are compared with the experimental values and the theoretical results deduced from the work of Kurucz (2017). These comparisons are illustrated in Figs. 5 and 6. It can be seen that our computed values are generally in better agreement with the experimental values (standard deviation $\Delta\sigma = 0.067$) than those from Kurucz (2017) ($\Delta\sigma = 0.089$). However, for two upper even levels, those located at $72\,125.247$ and $72\,183.090\text{ cm}^{-1}$, rather large discrepancies (up to two orders of magnitude) are observed when comparing the theoretical BFs with the measurements. This is mainly due to the strong mixings characterizing not only the upper but also the lower levels involved in the transitions. More precisely, according to our calculations, the main LS components of the levels at $72\,125.247$ and $72\,183.090\text{ cm}^{-1}$ are $81\% 5d\ ^5P_3 + 13\% 5d\ ^3D_3 + 2\% 5d\ ^5F_3$ and $60\% 5d\ ^5F_3 + 33\% 5d\ ^5G_3 + 2\% 5d\ ^3D_3$, respectively. Both of them have, for example, one transition to the $5p\ ^5F_3$ lower level ($E = 37\,376.901\text{ cm}^{-1}$), for which the theoretical and experimental BFs disagree. In fact, for this latter level, our calculations give a strongly mixed eigenvector, $53\% 5p\ ^5F_3 + 25\% 5p\ ^3D_3 + 7\% 5p\ ^5D_3$, giving rise to transition

decay rates for the lines at 2876.991 and 2872.209 \AA , which are very sensitive to small changes in the eigenvector compositions, both for the upper $5d$ and lower $5p$ levels. Moreover, both levels at $72\,125.247$ and $72\,183.090\text{ cm}^{-1}$ are depopulated by quite a large number of very weak lines (contributing to the residuals given in Table A.1), which are affected by strong cancellation effects in our calculations (see Cowan 1981). This makes the determination of BFs less reliable for these two levels.

4. Summary

We report experimental and theoretical radiative lifetimes for high lying even $4d^3\ 5d$ and $6s$ levels, between $68\,000$ and $73\,200\text{ cm}^{-1}$ in Nb II. In addition, we have measured BFs for 59 lines depopulating the levels. Combining the lifetimes with the BFs has generated absolute transition probabilities for the lines. The experimental values are compared with theoretical data, both new data reported in this work and values from the literature (Kurucz 2017).

Acknowledgements. This work was supported by the Swedish Research Council through the Linnaeus grant to the Lund Laser Centre and the Knut and Alice Wallenberg Foundation. This work was financially supported by the Integrated Initiative of Infrastructure Project LASERLAB-EUROPE, contract LLC002130. H.H acknowledges the Swedish Research Council Grant 2016-04185. P.P. and P.Q. are respectively Research Associate and Research Director of the Belgian Fund for Scientific Research F.R.S.-FNRS. Financial support from this organization is sincerely acknowledged.

References

- Corliss, C. H., & Bozman, W. R. 1962, *Natl. Bur. Stand. (US) Monogr.*, **53** (Washington, D.C.: US Department of Commerce)
- Cowan, R. D. 1981, *The Theory of Atomic Structure and Spectra* (Berkeley: Univ. California Press)
- Engström, L., Lundberg, H., Nilsson, H., Hartman, H., & Bäckström, E. 2014, *A&A*, **570**, A34
- Fraga, S., Karwowski, J., & Saxena, K. M. S. 1976, *Handbook of Atomic Data* (Amsterdam: Elsevier)
- Griffith, W. P., & Morris, P. J. T. 2003, *Notes Rec. R. Soc. Lond.*, **57**, 299
- Hannaford, P., Lowe, R. M., Biémont, E., & Grevesse, N. 1985, *A&A*, **143**, 447
- Humphreys, C. J., & Meggers, W. F. 1945, *Res. Nat. Bur. Stand. (U.S.)*, **43**, 481
- Iglesias, L. 1954, *An. Real Soc. Esp. Fys. Quim. (Madrid)*, **50**, 135
- Kurucz, R. L. 2017, Available at <http://kurucz.harvard.edu/atoms.html> [accessed June 18]
- Lundberg, H., Hartman, H., Engström, L., et al. 2016, *MNRAS*, **460**, 356
- Meggers, W. F., & Schribner, B. F. 1935, *J. Res. Natl. Bur. Stand. (U.S.)*, **14**, 629
- Mills, I., Cvitas, T., Homann, K., Kallay, N., & Kuchitsu, K. 1988, *Quantities, Units and Symbols in Physical Chemistry* (Oxford, UK: Blackwell Scientific Publications) [Copyright 1988 IUPAC]
- Nilsson, H., & Ivarsson, S. 2008, *A&A*, **492**, 609
- Nilsson, H., Hartman, H., Engström, L., et al. 2010, *A&A*, **511**, A16
- Neyskens, P., Van Eck, S., Jorissen, A., et al. 2015, *Nature*, **517**, 174
- Palmeri, P., Quinet, P., Fivet, V., et al. 2008, *Phys. Scr.*, **78**, 015304
- Quinet, P., Palmeri, P., Biémont, E., et al. 1999, *MNRAS*, **307**, 934
- Quinet, P., Palmeri, P., Biémont, E., et al. 2002, *J. Alloys Comp.*, **344**, 255
- Ryabtsev, A. N., Churilov, S. S., & Litzén, U. 2000, *Phys. Scr.*, **62**, 368
- Sikström, C. M., Nilsson, H., Litzén, U., Blom, A., & Lundberg, H. 2002, *J. Quant. Spectrosc. Radiat. Transfer*, **74**, 355
- Smith, V. V., & Lambert, D. L. 1984, *Publ. Astron. Soc. Pac.*, **96**, 226
- Whaling, W., Carle, M. T., & Pitt, M. L. 1993, *J. Quant. Spec. Radiat. Transf.*, **50**, 7
- Young, L., Hasegawa, S., Kurtz, C., Datta, D., & Beck, D. R. 1995, *Phys. Rev. A*, **51**, 3534

Appendix A: Additional table

Table A.1. Experimental and theoretical branching fractions for transitions in Nb II.

Upper level ^(a) [cm ⁻¹]	Lower level ^(a)	λ_{air} ^(a) [Å]	σ ^(a) [cm ⁻¹]	BF _{exp}	Unc [%]	BF _{theory}		log(<i>gf</i>) _{exp}	Unc _{gf} [%]
						This work	Kurucz ^(b)		
6s e ⁵ F ₅ <i>E</i> = 68 772.928	5p ⁵ G ₅	3002.242	33 298.731	0.0485	15	0.063	0.061	-0.549	16
	5p ⁵ G ₆	3093.403	32 317.471	0.5705	4	0.419	0.418	0.548	5
	5p ⁵ F ₄	3199.634	31 244.546	0.0308	16	0.064	0.071	-0.691	17
	5p ⁵ F ₅	3251.244	30 748.592	0.1982	12	0.195	0.193	0.132	12
	5p ⁵ D ₄	3279.714	30 481.676	0.1150	12	0.213	0.200	-0.097	13
	5p ³ G ₅	3396.035	28 669.323	0.0200	17	0.029	0.035	-0.826	18
Residual						0.017			
5d e ⁵ H ₃ <i>E</i> = 70 895.504	5p ⁵ G ₂	2662.720	37 544.414	0.9086	1	0.904	0.908	0.612	12
	5p ⁵ G ₃	2703.636	36 976.260	0.0514	7	0.056	0.042	-0.621	14
Residual						0.041			
5d e ⁵ P ₁ <i>E</i> = 70 995.981	5p ³ D ₁	2771.597	36 069.627	BL		0.078	0.135		
	5p ⁵ D ₀	2970.218	33 657.739	0.1625	18	0.177	0.153	-0.513	20
	5p ⁵ D ₁	2986.352	33 475.905	0.4570	12	0.422	0.402	-0.059	14
	5p ⁵ D ₂	3014.925	33 158.665	0.2365	16	0.257	0.215	-0.337	17
Residual						0.144			
5d e ⁵ F ₁ <i>E</i> = 71 196.067	5p ³ D ₁	2753.270	36 309.713	0.4332	16	0.446	0.424	-0.173	18
	5p ³ D ₂	2802.238	35 675.245	0.0993	18	0.117	0.102	-0.797	19
	5p ⁵ D ₀	2949.180	33 897.825	0.1555	22	0.125	0.166	-0.558	23
Residual						0.313			
5d e ⁵ H ₅ <i>E</i> = 71 684.873	5p ⁵ G ₄	2698.048	37 052.967	0.8796	1	0.881	0.858	0.734	8
	5p ⁵ G ₅	2760.801	36 210.803	0.0263	7	0.033	0.020	-0.771	10
	5p ⁵ F ₄	2926.845	34 156.618	0.0771	7	0.069	0.095	-0.253	11
Residual						0.018			
5d e ⁵ P ₃ <i>E</i> = 72 125.247	5p ⁵ G ₄	2666.356	37 493.214	0.0595	6	0.001	0.047	-0.654	10
	5p ³ D ₂	2731.102	36 604.425	0.0813	6	0.028	0.008	-0.497	10
	5p ⁵ F ₂	2843.105	35 162.473	0.0126	22	0.013	0.009	-1.273	23
	5p ⁵ F ₃	2876.991	34 748.346	0.3501 ^(c)	15	0.130	0.003	0.182	17
	5p ⁵ F ₄	2889.588	34 596.865	0.0482	9	0.024	0.002	-0.676	12
	5p ⁵ D ₂	2912.227	34 327.931	0.1126	7	0.038	0.004	-0.300	10
5p ⁵ D ₄	2954.744	33 833.995	0.3359	6	0.617	0.418	0.187	10	
Residual ^(d)						0.150			
5d e ⁵ F ₃ <i>E</i> = 72 183.090	5p ⁵ G ₃	2612.653	38 263.846	0.0452	3	0.079	0.065	-0.811	8
	5p ⁵ G ₄	2662.249	37 551.057	0.1077	3	0.148	0.096	-0.417	8
	5p ³ D ₃	2805.809	35 629.852	0.4720	2	0.374	0.076	0.270	8
	5p ⁵ F ₃	2872.209	34 806.189	0.0307	12	0.135	0.317	-0.896	14
	5p ⁵ F ₄	2884.765	34 654.708	0.0300	12	0.067	0.068	-0.903	14
	5p ⁵ D ₂	2907.328	34 385.774	0.0354	13	0.106	0.150	-0.824	15
	5p ⁵ D ₃	2943.199	33 966.703	0.0750	9	0.035	0.000	-0.487	12
	5p ⁵ D ₄	2949.701	33 891.838	0.2041	5	0.011	0.116	-0.051	9
Residual ^(d)						0.045			
5d e ⁵ H ₆ <i>E</i> = 72 231.658	5p ⁵ G ₅	2719.730	36 757.461	0.9057	1	0.910	0.894	0.826	8
	5p ⁵ G ₆	2794.330	35 776.201	0.0168	8	0.016	0.010	-0.883	11
	5p ⁵ F ₅	2922.495	34 207.322	0.0725	7	0.069	0.091	-0.208	11
Residual						0.004			

Notes. ^(c)Corrected for blend (see text). ^(d)Residual not included in these levels (see text).

References. ^(a)Ryabtsev et al. (2000). ^(b)Kurucz (2017).

Table A.2. continued.

Upper level ^(a) [cm ⁻¹]	Lower level ^(a)	λ_{air} ^(a) [Å]	σ ^(a) [cm ⁻¹]	BF _{exp}	Unc [%]	BF _{theory}		log(gf) _{exp}	Unc _{gf} [%]
						This work	Kurucz ^(b)		
5d e ⁵ G ₅ E = 72 460.669	5p ⁵ G ₄	2642.713	37 828.636	0.0455	4	0.026	0.063	-0.613	10
	5p ⁵ G ₅	2702.889	36 986.472	0.3307	3	0.295	0.311	0.278	10
	5p ⁵ F ₄	2861.841	34 932.287	0.3975	3	0.410	0.361	0.408	10
	5p ⁵ F ₅	2903.059	34 436.333	0.0719	5	0.085	0.071	-0.323	11
	5p ⁵ D ₄	2925.737	34 169.417	0.1315	4	0.160	0.167	-0.053	10
Residual						0.024			
5d e ⁵ F ₄ E = 72 624.931	5p ⁵ G ₄	2631.286	37 992.898	0.1099	3	0.115	0.109	-0.289	8
	5p ⁵ G ₅	2690.938	37 150.734	0.1548	3	0.131	0.124	-0.121	8
	5p ³ D ₃	2771.439	36 071.693	0.0725	4	0.065	0.075	-0.425	8
	5p ⁵ F ₄	2848.446	35 096.549	0.4833	2	0.502	0.489	0.423	8
	5p ⁵ F ₅	2889.276	34 600.595	0.0244	9	0.028	0.020	-0.862	12
	5p ⁵ D ₃	2905.404	34 408.544	0.1097	4	0.116	0.123	-0.204	9
Residual						0.020			
5d e ⁵ H ₇ E = 72 861.270	5p ⁵ G ₆	2746.002	36 405.813	1.0000		1.000	0.998	0.987	6
Residual						0.000			
5d e ⁵ F ₅ E = 73 115.352	5p ⁵ G ₅	2655.876	37 641.073	0.1646	3	0.130	0.114	-0.008	8
	5p ⁵ G ₆	2726.969	36 659.813	0.1011	3	0.096	0.094	-0.196	8
	5p ⁵ F ₄	2809.190	35 586.888	0.0659	4	0.068	0.068	-0.357	9
	5p ⁵ F ₅	2848.895	35 090.934	0.4537	2	0.480	0.475	0.494	8
	5p ⁵ D ₄	2870.732	34 824.018	0.1551	4	0.160	0.175	0.034	9
	5p ³ G ₅	3028.343	33 011.665	0.0465	16	0.053	0.055	-0.442	18
Residual						0.013			
5d e ⁵ G ₆ E = 73 161.143	5p ⁵ G ₅	2652.649	37 686.946	0.0542	4	0.027	0.055	-0.451	10
	5p ⁵ G ₆	2723.567	36 705.686	0.4190	3	0.409	0.404	0.460	10
	5p ⁵ F ₅	2845.182	35 136.807	0.4929	3	0.529	0.505	0.569	10
	5p ³ G ₅	3024.148	33 057.538	0.0329	14	0.034	0.028	-0.554	17
Residual						0.011			